Degradation of ATFS-1 by LONP-1 promotes deleterious mitochondrial genome heteroplasmy

Authors:

Qiyuan Yang[1], Pengpeng Liu[1], YunGuang Du[1], Kevin Luk[1], Nadine S. Anderson[1], Josh Lavelle[1], Rilee D. Zeinert[2,3], Peter Chien[2,3], Scot A. Wolfe[1], Cole M. Haynes[1]*

Affiliations:

[1]Department of Molecular, Cell and Cancer Biology, University of Massachusetts Medical School, Worcester, MA 01605, USA.

[2]Department of Biochemistry and Molecular Biology, University of Massachusetts Amherst, MA 01002, USA

[3]Molecular and Cellular Biology Graduate Program, University of Massachusetts Amherst, MA 01002, USA

*Correspondence to: cole.haynes@umassmed.edu

One Sentence Summary:

The mitochondrial protease LONP1 regulates deleterious mitochondrial genome propagation.

Abstract:

The accumulation of deleterious mitochondrial genomes (ΔmtDNAs) underlies inherited mitochondrial diseases and contributes to the aging-associated decline in mitochondrial function. Heteroplasmy occurs when a ΔmtDNA expands, ultimately causing a decline in oxidative phosphorylation (OXPHOS) function. In response to mitochondrial perturbations, the transcription factor ATFS-1 induces a transcription program to promote cell survival and recovery of mitochondrial function. Paradoxically, ATFS-1 is also required to maintain ΔmtDNAs in heteroplasmic worms. However, the mechanism(s) by which ATFS-1 promotes ΔmtDNA propagation relative to wild-type mtDNAs is unclear. Here, we show that mitochondrial-localized ATFS-1 binds almost exclusively to ΔmtDNAs in heteroplasmic worms and promotes binding of the mtDNA replicative polymerase (POLG). Interestingly, inhibition of the mtDNA-bound protease LONP-1 caused ATFS-1 and POLG to bind equally to ΔmtDNAs and wild-type mtDNAs. Furthermore, LONP-1 inhibition in *C. elegans* and human cybrid cells improved the heteroplasmy ratio and restored OXPHOS function. Our findings suggest that degradation of ATFS-1 within functional mitochondria by LONP-1 establishes the enriched interaction between ATFS-1 and ΔmtDNAs required to maintain heteroplasmy.

mtDNAs encode proteins required for oxidative phosphorylation (OXPHOS). Heteroplasmy occurs when a deleterious mutant mtDNA clone expands to a high enough percentage relative to wild-type mtDNAs to perturb OXPHOS function. Interestingly, expression of mitochondrial-targeted nucleases that specifically cleave deleterious mtDNAs suggest that a modest reduction in the ratio of mutant to wild-type mtDNA is sufficient to improve mitochondrial function (*1, 2*). Mitophagy has been shown to limit the accumulation of ∆mtDNAs by specifically degrading dysfunctional mitochondria, which likely harbor ∆mtDNAs (*3*). ∆mtDNA propagation is also suppressed by a mechanism that limits protein synthesis on the outer membrane of dysfunctional mitochondria (*4*). However, the mechanisms that amplify clonal deleterious mtDNAs and maintain them at a high enough percentage to cause OXPHOS defects in mitochondrial diseases (*5-8*), aging (*9*) and Parkinson's Disease (*10*) remain unclear.

The UPR^{mt} transcription factor ATFS-1 is required to maintain ∆mtDNAs (*11, 12*) in a heteroplasmic *C. elegans* strain that harbors ~60% ∆mtDNAs with a 3.1kb deletion (*13*). ATFS-1 harbors both a nuclear localization sequence (NLS) and a mitochondrial targeting sequence (MTS) (Fig. 1A), consistent with biochemical fractionation evidence indicating that this bZIP protein resides in both compartments. In wild-type worms, the majority of ATFS-1 is imported into the mitochondrial matrix where it is degraded by the protease LONP-1 (Fig. 1A) (*14, 15*). However, during mitochondrial dysfunction caused by inhibition of the essential mitochondrial protease SPG-7, ATFS-1 accumulates in the nucleus (*16*) where it mediates a transcriptional response known as the mitochondrial unfolded protein response (UPR^{mt}) to promote survival, longevity and recovery of mitochondrial function (*17*). Importantly, ATFS-1 also accumulates within the

mitochondrial matrix where it binds mtDNA at a single site within the regulatory non-coding region (NCR) (Fig. 1B) (*15*). Both mitochondrial and nuclear accumulation of ATFS-1 are required for development during mitochondrial dysfunction (*11, 15*). Because ATFS-1 binds mtDNA and induces over 600 mRNAs during mitochondrial dysfunction, it is unclear whether ATFS-1 promotes heteroplasmy by suppressing degradation of ΔmtDNAs or by stimulating ΔmtDNA replication.

Consistent with heteroplasmy causing mitochondrial dysfunction (*18*), mitochondrial membrane potential was reduced in heteroplasmic worms relative to wild-type worms (Figs. 1C,D) although not to the extent of wild-type worms raised on *spg-7*(RNAi) (Figs. 1C,D). As in *spg-7*(RNAi)-treated worms, ATFS-1 accumulated within mitochondria of heteroplasmic worms as determined by subcellular fractionation (Fig. 1E). As ATFS-1 binds mtDNA during mitochondrial dysfunction, we examined the interaction with mtDNA in heteroplasmic worms via IP-mtDNA followed by qPCR to quantify total, wild-type and ΔmtDNAs (Fig. 1F). While heteroplasmic worms harbored 1.25-fold more mtDNAs than wild-type worms (fig. S1A), ATFS-1 interacted with ~6-fold more mtDNAs in heteroplasmic worms relative to wild-type homoplasmic worms (Fig. 1G), consistent with the accumulation of ATFS-1 in dysfunctional mitochondria (Fig. 1E). Because the ATFS-1 binding site within the NCR is present in both wild-type mtDNA and ΔmtDNA, we examined binding to each genome. Strikingly, of the mtDNAs bound by ATFS-1, 91.8% were ΔmtDNAs and 8.2% were wild-type mtDNAs, which is considerably enriched relative to the ΔmtDNA ratio of 59% in whole worm lysate (Fig. 1H).

Previously, we found that inhibition of the mtDNA replicative polymerase POLG caused depletion of ΔmtDNAs in heteroplasmic worms relative to wild-type mtDNAs (*11*),

which is similar to findings in a *Drosophila* model of deleterious mtDNA heteroplasmy (*19*). Both findings suggest increased replication of ΔmtDNAs in heteroplasmic cells. To explore the relationship between ATFS-1 and mtDNA replication, we generated POLG antibodies which detected a ~120 KD band that co-fractionated with the OXPHOS protein NDUFS3 (fig. S1B) and was depleted by *polg*(RNAi) (fig. S1C). Interestingly, IP-mtDNA using the POLG antibody indicated that the replicative polymerase also interacted with more ΔmtDNAs than wildtype mtDNAs (Fig. 1I and fig. S1D), similar to ATFS-1 (Fig. 1H). As a control, we generated antibodies to the mtDNA packaging protein HMG-5 (TFAM in mammals) (figs. S1E,F), which interacts with mtDNAs independent of replication (*20*). In contrast to ATFS-1 and POLG, the percentage of ΔmtDNAs bound to HMG-5 reflected the percentage within the whole worm lysate (fig. S1G). Combined, these data indicate that ATFS-1 and a component of the replisome preferentially associate with ΔmtDNAs relative to wild-type mtDNAs in heteroplasmic worms.

To further examine the role of mitochondrial-localized ATFS-1 in maintaining heteroplasmy, we generated a strain in which the NLS within ATFS-1 was impaired via genome editing (Fig. 2A and fig. S2A). Consistent with *atfs-1*$^{\Delta NLS}$ lacking nuclear activity, induction of *hsp-6* mRNA was impaired when raised on *spg-7*(RNAi) (fig. S2B). The ΔNLS mutation also suppressed activation of the UPR^{mt} reporter *hsp-6*$_{pr}$*::gfp*, and *hsp-6* mRNA, caused by an allele of ATFS-1 with a weak mitochondrial targeting sequence that causes constitutive UPR^{mt} activation (*21*) (Figs. 2B,C). Importantly, ATFS-1$^{\Delta NLS}$ accumulated within mitochondria to similar levels as wild-type ATFS-1 upon LONP-1 inhibition (Fig. 2D) indicating the protein was expressed and processed similarly to wild-type ATFS-1. We next introduced the *atfs-1(null)* (*22*) or *atfs-1*$^{\Delta NLS}$ alleles into heteroplasmic worms. As

expected, *atfs-1(null)* worms were unable to harbor any ΔmtDNAs (Fig. 2E). However, despite the lack of the *atfs-1*-mediated nuclear transcription program, *atfs-1*$^{\Delta NLS}$ worms were able to maintain ΔmtDNAs, albeit to a somewhat lesser degree than wild-type *atfs-1* worms (Fig. 2E). Like ATFS-1, ATFS-1$^{\Delta NLS}$ also bound a higher percentage of ΔmtDNAs, consistent with mitochondrial-localized ATFS-1 being sufficient to maintain heteroplasmy (Figs. 2E,F). Combined, these findings emphasize the importance of mitochondrial-localized ATFS-1 in maintaining deleterious mtDNA heteroplasmy.

We next sought to determine if mitochondrial-localized ATFS-1 is required for POLG binding to mtDNA in dysfunctional mitochondria. Because *atfs-1*-deletion caused complete loss of ΔmtDNAs in heteroplasmic worms (Fig. 2E), we examined the dependence of the POLG-mtDNA interaction on ATFS-1 in homoplasmic worms raised on control or *spg-7*(RNAi) (Fig. 2G). Similar to ATFS-1 (Fig. 1B), POLG interacted with more mtDNAs during exposure to *spg-7*(RNAi) (Fig. 2G). However, POLG binding to mtDNA was reduced in *atfs-1(null)* worms (Fig. 2G), suggesting ATFS-1 promotes POLG binding to mtDNAs in dysfunctional mitochondria. To circumvent the potentially confounding effects of the induction of *polg* mRNA by ATFS-1 during stress (*11, 16*), we performed a similar experiment in *atfs-1*$^{\Delta NLS}$ worms that lack nuclear activity. Like wild-type ATFS-1, ATFS-1$^{\Delta NLS}$ also promoted POLG binding to mtDNA during *spg-7*(RNAi) exposure, in contrast to *atfs-1(null)* worms (fig. S2C). Combined, our data suggest that ATFS-1 accumulation within dysfunctional mitochondria promotes POLG recruitment to mtDNA.

To gain insight into how the enriched association between ATFS-1 and ΔmtDNAs is established in heteroplasmic worms, we focused on the mitochondrial protease LONP-

1, which is required for the degradation of ATFS-1 within the mitochondrial matrix of wild-type worms (Figs. 1A and 2D) (*16*). LONP-1 is known to interact with mtDNA in diverse species (*23, 24*), and has been shown to regulate mtDNA replication (*25, 26*), suggesting a role in regulating heteroplasmy. We generated antibodies to *C. elegans* LONP-1 (fig. S3A), as well as a strain in which the C-terminus of LONP-1 was epitope tagged via genome editing (figs. S3B,C,D,E). As expected, LONP-1 interacted with mtDNA in *C. elegans* (Fig. 3A, S4A) And, unlike ATFS-1, LONP-1 interacted similarly with wildtype and ∆mtDNAs (fig. S4B) suggesting LONP-1 is constitutively bound while ATFS-1 binding is likely transient. Lastly, we sought to determine where in the mtDNA LONP-1^{FLAG} binds. LONP-1^{FLAG} ChIP-seq indicated that LONP-1 bound several G-rich sites throughout mtDNA (fig. S4C), but was especially enriched within the NCR (Fig. 3B). Interestingly, the strongest LONP-1^{FLAG} peak within the NCR overlapped with the ATFS-1 binding site (Fig. 3B and fig. S4D) suggesting it may regulate ATFS-1 binding to mtDNA.

We next examined the interaction between ATFS-1 and mtDNAs in heteroplasmic worms upon LONP-1 inhibition. As before, ATFS-1 binding was enriched on ∆mtDNAs (Fig. 3C). However, *lonp-1*(RNAi) exposure resulted in ATFS-1 binding nearly equally to wild-type mtDNAs and ∆mtDNAs indicating the mtDNA-bound protease is required for the enriched interaction between ATFS-1 and ∆mtDNAs (Fig. 3C). Interestingly, *lonp-1* inhibition via RNAi caused a 2-fold reduction of ∆mtDNAs (Fig 3D) and a concomitant increase in wild-type mtDNAs improving the heteroplasmy ratio from 61% ∆mtDNAs to 28.7% (Fig. 3D). Similar results were obtained in *atfs-1*$^{\Delta NLS}$ worms upon LONP-1 inhibition (fig. S5A). In addition to increasing the percentage of wild-type mtDNAs bound by ATFS-1, *lonp-1*(RNAi) also increased the percentage of POLG that interacted with wild-type

mtDNAs while reducing the amount bound to ΔmtDNAs (Fig. 3E). Importantly, *lonp-1*(RNAi) did not alter the percentage of HMG-5/TFAM bound to ΔmtDNAs, consistent with HMG-5 interacting with all mtDNAs (fig. S5B). Combined, these findings support a role for LONP-1-mediated degradation of mitochondrial ATFS-1 in promoting ΔmtDNA propagation.

We next examined the impact of *lonp-1*(RNAi) on mtDNA accumulation in homoplasmic worms. Exposure to *lonp-1*(RNAi) resulted in increased ATFS-1 binding to mtDNA (Fig. 3F) and an increase in total mtDNA (Fig. 3G), suggesting the ATFS-1:mtDNA interaction promotes replication. Furthermore, *lonp*-1(RNAi) also caused increased POLG:mtDNA binding (Fig. 3H). Moreover, in *atfs-1*$^{\Delta NLS}$ worms, LONP-1 inhibition also increased total mtDNA number (fig. S5C). However, the increase in mtDNA caused by LONP-1 inhibition was abolished in *atfs-1(null)* worms (Fig. 3G). Together, these findings support a role for mitochondrial-localized ATFS-1 in promoting mtDNA replication in a manner that is negatively regulated by LONP-1-dependent degradation of ATFS-1.

Lastly, we examined if the role of LONP1 in maintaining ΔmtDNAs is conserved in mammals by examining two human heteroplasmic cybrid cell lines, which harbor a combination of wild-type mtDNA and ΔmtDNAs associated with mitochondrial disease (*27*). One cybrid line harbors a single nucleotide transition (COXI G6930A) that introduces a premature stop codon in the cytochrome c oxidase subunit I gene isolated from a patient with a multisystem mitochondrial disorder (*28*). We also examined a cybrid line harboring a 4977 base pair deletion known as the “common deletion” which removes multiple OXPHOS genes and is associated with Kearns-Sayre Syndrome (KSS), progressive external ophthalmoplegia, cancer and aging (*29-32*). We first examined the impact of

LONP1 siRNA on heteroplasmy in the KSS cybrid line. Similar to inhibition of *C. elegans* LONP-1, inhibition of human LONP1 by siRNA for 4 days (fig. S6A) improved the heteroplasmy ratio from 56.9% to 27.6% KSS mtDNA (Fig. 4A). Similarly, ∆mtDNAs were decreased 2.7-fold suggesting LONP1's role in promoting heteroplasmy is conserved in mammals (Fig. 4B).

To further investigate the role of LONP1 protease activity, we used the LONP1 inhibitor CDDO (2-cyano-3,12-dioxo-oleana-1,9(11)-dien-28-oic acid), also known as Bardoxolone (*33*). 0.1 μM and 0.25 μM CDDO were used, as neither concentration affected viability of the KSS or CoxI G6930A cell lines (Fig. 4C and fig. S6B). As determined by deep sequencing, the CoxI G6930A cybrid line initially harbored 86% G6930A mutant mtDNA and 14% wild-type mtDNA (Fig. 4D and fig. S6C). Impressively, incubation with 0.1 μM or 0.25 μM CDDO for 3 weeks resulted in depletion of the CoxI G6930A mtDNA from 86% to 68% and 72%, respectively, with a relative increase in wild-type mtDNAs (Fig. 4D and fig. S6C), Furthermore, continuous incubation with 0.1μM or 0.25 μM CDDO for 18.5 weeks further decreased the heteroplasmic ratios from ~90% to ~47% and 62%, respectively (Fig. 4D and fig. S6C). Mitochondrial respiratory function was also measured at time points throughout the time course (Figs. 4E-G). Impressively, depletion of the CoxI G6930A mtDNA resulted in increased basal respiration and maximal respiratory capacity (Figs. 4E-G). For example, 3 weeks exposure to 0.1 μM CDDO improved basal oxygen consumption ~2-fold (Figs. 4E,F), while exposure for 18.5 weeks improved basal oxygen consumption over 3-fold (Figs. 4E,F).

Similar results were obtained when the KSS cybrid cells were incubated with CDDO. As determined by qPCR, KSS cells initially harbored ~50% ∆mtDNA. Incubation

with 0.1 µM or 0.25 µM CDDO for 4 weeks depleted ∆mtDNAs to 19.6% and 21.2%, respectively, alongside a concomitant ~2-fold increase in basal oxygen consumption (figs. S6D,E). These findings suggest that LONP1 promotes propagation of deleterious mtDNAs independent of genome length, as maintenance of mutant mtDNAs with either a large deletion or a single base pair substitution require LONP1 function.

In summary, these results demonstrate that degradation of mitochondrial-localized ATFS-1 by the protease LONP-1 regulates the propagation of deleterious mtDNAs. We propose that under basal conditions, this mechanism enables compartment-autonomous regulation of mtDNA replication that responds to functional heterogeneity within the mitochondrial network. In such a model, a decline in mitochondrial function would be accompanied by impaired LONP1 activity, resulting in accumulation of ATFS-1 within mitochondria, increased binding of ATFS-1 to mtDNA, and recruitment of the replisome to mtDNA. However, if compartmental dysfunction arises because of ∆mtDNAs, these deleterious genomes are preferentially replicated. Inhibiting LONP1 throughout the mitochondrial network may negate this preferential replication, leading to a reduction in the heteroplasmic ratio and recovery of mitochondrial function

References and Notes

1. S. Srivastava, C. T. Moraes, Manipulating mitochondrial DNA heteroplasmy by a mitochondrially targeted restriction endonuclease. *Human molecular genetics* **10**, 3093-3099 (2001).
2. M. Tanaka *et al.*, Gene therapy for mitochondrial disease by delivering restriction endonucleaseSmaI into mitochondria. *Journal of biomedical science* **9**, 534-541 (2002).
3. D. F. Suen, D. P. Narendra, A. Tanaka, G. Manfredi, R. J. Youle, Parkin overexpression selects against a deleterious mtDNA mutation in heteroplasmic cybrid cells. *Proceedings of the National Academy of Sciences of the United States of America* **107**, 11835-11840 (2010).
4. Y. Zhang *et al.*, PINK1 inhibits local protein synthesis to limit transmission of deleterious mitochondrial DNA mutations. *Molecular cell* **73**, 1127-1137. e1125 (2019).
5. A. Hahn, S. Zuryn, The Cellular Mitochondrial Genome Landscape in Disease. *Trends Cell Biol* **29**, 227-240 (2019).
6. C. V. Pereira, C. T. Moraes, Current strategies towards therapeutic manipulation of mtDNA heteroplasmy. *Front Biosci (Landmark Ed)* **22**, 991-1010 (2017).
7. N. G. Larsson, D. A. Clayton, Molecular genetic aspects of human mitochondrial disorders. *Annu Rev Genet* **29**, 151-178 (1995).
8. E. A. Schon, S. DiMauro, M. Hirano, R. W. Gilkerson, Therapeutic prospects for mitochondrial disease. *Trends Mol Med* **16**, 268-276 (2010).
9. L. C. Greaves *et al.*, Clonal expansion of early to mid-life mitochondrial DNA point mutations drives mitochondrial dysfunction during human ageing. *PLoS genetics* **10**, e1004620 (2014).
10. A. Bender *et al.*, High levels of mitochondrial DNA deletions in substantia nigra neurons in aging and Parkinson disease. *Nature genetics* **38**, 515-517 (2006).
11. Y. F. Lin *et al.*, Maintenance and propagation of a deleterious mitochondrial genome by the mitochondrial unfolded protein response. *Nature* **533**, 416-419 (2016).
12. B. L. Gitschlag *et al.*, Homeostatic Responses Regulate Selfish Mitochondrial Genome Dynamics in C. elegans. *Cell Metab* **24**, 91-103 (2016).
13. W. Y. Tsang, B. D. Lemire, Stable heteroplasmy but differential inheritance of a large mitochondrial DNA deletion in nematodes. *Biochem Cell Biol* **80**, 645-654 (2002).
14. A. M. Nargund, M. W. Pellegrino, C. J. Fiorese, B. M. Baker, C. M. Haynes, Mitochondrial import efficiency of ATFS-1 regulates mitochondrial UPR activation. *Science* **337**, 587-590 (2012).
15. A. M. Nargund, C. J. Fiorese, M. W. Pellegrino, P. Deng, C. M. Haynes, Mitochondrial and nuclear accumulation of the transcription factor ATFS-1 promotes OXPHOS recovery during the UPR(mt). *Molecular cell* **58**, 123-133 (2015).
16. A. M. Nargund, M. W. Pellegrino, C. J. Fiorese, B. M. Baker, C. M. Haynes, Mitochondrial import efficiency of ATFS-1 regulates mitochondrial UPR activation. *Science* **337**, 587-590 (2012).

17. T. Shpilka, C. M. Haynes, The mitochondrial UPR: mechanisms, physiological functions and implications in ageing. *Nature reviews. Molecular cell biology* **19**, 109-120 (2018).
18. Y. F. Lin *et al.*, Maintenance and propagation of a deleterious mitochondrial genome by the mitochondrial unfolded protein response. *Nature*, (2016).
19. A. C.-Y. Chiang, E. McCartney, P. H. O'Farrell, H. Ma, A genome-wide screen reveals that reducing mitochondrial DNA polymerase can promote elimination of deleterious mitochondrial mutations. *Current Biology* **29**, 4330-4336. e4333 (2019).
20. C. Kukat *et al.*, Cross-strand binding of TFAM to a single mtDNA molecule forms the mitochondrial nucleoid. *Proc Natl Acad Sci U S A* **112**, 11288-11293 (2015).
21. M. Rauthan, P. Ranji, N. Aguilera Pradenas, C. Pitot, M. Pilon, The mitochondrial unfolded protein response activator ATFS-1 protects cells from inhibition of the mevalonate pathway. *Proceedings of the National Academy of Sciences of the United States of America* **110**, 5981-5986 (2013).
22. P. Deng *et al.*, Mitochondrial UPR repression during Pseudomonas aeruginosa infection requires the bZIP protein ZIP-3. *Proceedings of the National Academy of Sciences of the United States of America*, (2019).
23. T. Liu *et al.*, DNA and RNA binding by the mitochondrial lon protease is regulated by nucleotide and protein substrate. *The Journal of biological chemistry* **279**, 13902-13910 (2004).
24. S. H. Chen, C. K. Suzuki, S. H. Wu, Thermodynamic characterization of specific interactions between the human Lon protease and G-quartet DNA. *Nucleic acids research* **36**, 1273-1287 (2008).
25. Y. Matsushima, Y. I. Goto, L. S. Kaguni, Mitochondrial Lon protease regulates mitochondrial DNA copy number and transcription by selective degradation of mitochondrial transcription factor A (TFAM). *Proceedings of the National Academy of Sciences* **107**, 18410-18415 (2010).
26. A. Göke *et al.*, Mrx6 regulates mitochondrial DNA copy number in S. cerevisiae by engaging the evolutionarily conserved Lon protease Pim1. *Molecular Biology of the Cell*, mbc.E19-08-0470 (2019).
27. M. P. King, G. Attardi, Human cells lacking mtDNA: repopulation with exogenous mitochondria by complementation. *Science* **246**, 500-503 (1989).
28. C. Bruno *et al.*, A stop-codon mutation in the human mtDNA cytochrome c oxidase I gene disrupts the functional structure of complex IV. *Am J Hum Genet* **65**, 611-620 (1999).
29. C. T. Moraes *et al.*, Mitochondrial DNA deletions in progressive external ophthalmoplegia and Kearns-Sayre syndrome. *N Engl J Med* **320**, 1293-1299 (1989).
30. C. T. Moraes, E. A. Schon, S. DiMauro, A. F. Miranda, Heteroplasmy of mitochondrial genomes in clonal cultures from patients with Kearns-Sayre syndrome. *Biochem Biophys Res Commun* **160**, 765-771 (1989).
31. A. A. M. Yusoff, W. S. W. Abdullah, S. Khair, S. M. A. Radzak, A comprehensive overview of mitochondrial DNA 4977-bp deletion in cancer studies. *Oncol Rev* **13**, 409 (2019).

32. H. C. Lee, C. Y. Pang, H. S. Hsu, Y. H. Wei, Differential accumulations of 4,977 bp deletion in mitochondrial DNA of various tissues in human ageing. *Biochim Biophys Acta* **1226**, 37-43 (1994).
33. S. H. Bernstein *et al.*, The mitochondrial ATP-dependent Lon protease: a novel target in lymphoma death mediated by the synthetic triterpenoid CDDO and its derivatives. *Blood* **119**, 3321-3329 (2012).

Acknowledgments: We thank the Caenorhabditis Genetics Center for providing *C. elegans* strains (funded by NIH Office of Research 362 Infrastructure Programs (P40 OD010440). We thank Carlos Moraes for the KSS and Giovanni Manfredi for the CoxI G6930A cybrid cell lines. **Funding:** This work was supported by HHMI, the Mallinckrodt Foundation and National Institutes of Health grants (R01AG040061 and R01AG047182) to C.M.H., (R01GM115911 and R01AI117839) to S.A.W., (R01GM111706 and R35GM130320) to P.C. and (F31HL147482) to K.L. **Author contributions:** Q.Y. and C.M.H. planned the experiments. Q.Y., Y.D., R.C., and P.C. generated the worm strains. Q.Y. performed the *C. elegans* and cybrid mtDNA analysis including ChIP and respiratory function. P.L., K.L. and S.W. performed and analysed mtDNA sequencing. Q.Y., N.S.A. and C.M.H. wrote the manuscript. **Competing interests:** The authors declare no competing financial interests. **Data and materials availability:** All data in the paper are present in the paper or the Supplementary Materials. The ChIP-sequencing data have been deposited to the Gene Expression Omnibus database under the BioProject accession code PRJNA590136. The next-generation sequencing data have been deposited in the NCBI Sequence Read Archive database under the BioProject accession code PRJNA517630.

Supplementary Materials:

Materials and Methods

Figures S1-S6

Tables S1-S2 (.xlsx)

References

Fig. 1.

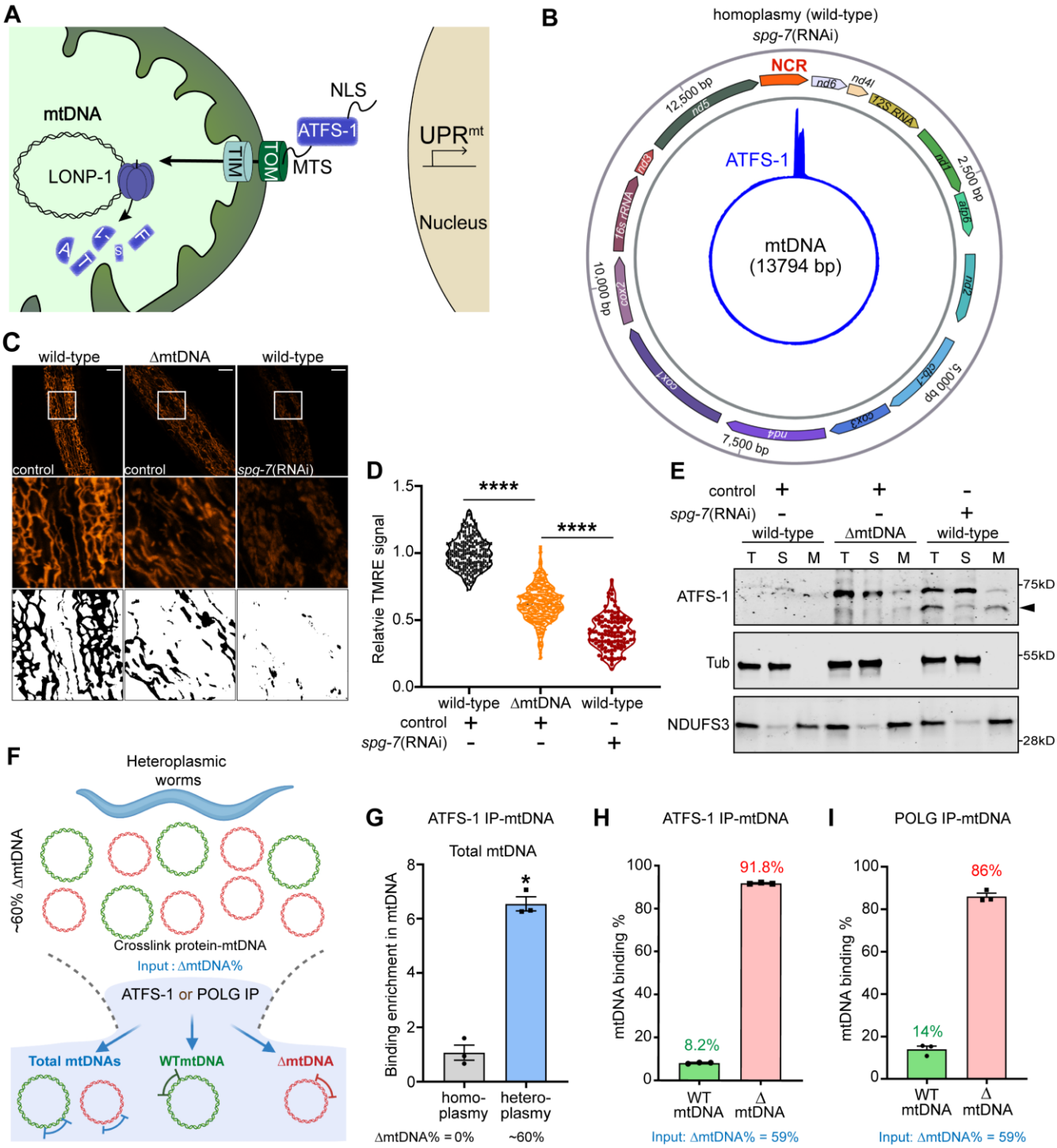
A
mtDNA
LONP-1
NLS
ATFS-1
TIM
TOM
MTS
UPRmt
Nucleus
B
homoplasmy (wild-type)
spg-7(RNAi)
NCR
ATFS-1
mtDNA
(13794 bp)
12,500 bp
2,500 bp
5,000 bp
7,500 bp
10,000 bp
C
wild-type
ΔmtDNA
wild-type
control
control
spg-7(RNAi)
D
Relatvie TMRE signal
****
****
wild-type
ΔmtDNA
wild-type
control
spg-7(RNAi)
E
control
spg-7(RNAi)
wild-type
ΔmtDNA
wild-type
T S M T S M T S M
ATFS-1
Tub
NDUFS3
75kD
55kD
28kD
F
Heteroplasmic worms
~60% ΔmtDNA
Crosslink protein-mtDNA
Input : ΔmtDNA%
ATFS-1 or POLG IP
Total mtDNAs
WTmtDNA
ΔmtDNA
G
ATFS-1 IP-mtDNA
Total mtDNA
Binding enrichment in mtDNA
homo-plasmy
hetero-plasmy
ΔmtDNA% = 0%
~60%
H
ATFS-1 IP-mtDNA
mtDNA binding %
8.2%
91.8%
WT mtDNA
Δ mtDNA
Input: ΔmtDNA% = 59%
I
POLG IP-mtDNA
mtDNA binding %
14%
86%
WT mtDNA
Δ mtDNA
Input: ΔmtDNA% = 59%

Fig. 1. Enriched binding of ATFS-1 and POLG to ∆mtDNAs in heteroplasmic worms. (**A**) ATFS-1/UPR^{mt} signaling schematic. (**B**) ATFS-1 ChIP-seq profile of the entire mitochondrial genome (mtDNA) of wild-type worms raised on *spg-7*(RNAi). (**C** and **D**) Images of TMRE-stained micrographs (C) and TMRE quantification (D) of wild-type and heteroplasmic(∆mtDNA) worms raised on control(RNAi) or wild-type worms raised on *spg-7*(RNAi). Scale bar, 10 µm. (**E**) Immunoblots of wild-type and ∆mtDNA worms raised on control(RNAi) or wild-type worms raised on *spg-7*(RNAi) after fractionation into total lysate (T), post-mitochondrial supernatant (S), and mitochondrial pellet (M). Tubulin (Tub) and the OXPHOS component (NDUFS3) are used as loading controls. Arrow is mitochondrial-localized ATFS-1. (**F**) Workflow of ATFS-1 or POLG IP-mtDNA and quantification of wild-type mtDNA, ∆mtDNA and total mtDNAs in heteroplasmic worms. (**G**) Quantification of total mtDNA following ATFS-1 IP-mtDNA in wild-type homoplasmic or heteroplasmic worms. (**H)** Quantification of wild-type mtDNA and ∆mtDNA following ATFS-1 IP-mtDNA in heteroplasmic worms. Post-lysis/Input ∆mtDNA ratio was 59%. (**I**) Quantification of wild-type mtDNA and ∆mtDNA following POLG IP-mtDNA in heteroplasmic worms. Post-lysis/Input ∆mtDNA ratio was 59%. n = 3; error bars mean ± S.E.M.; *p<0.05 (Student's t-test).

Fig. 2.

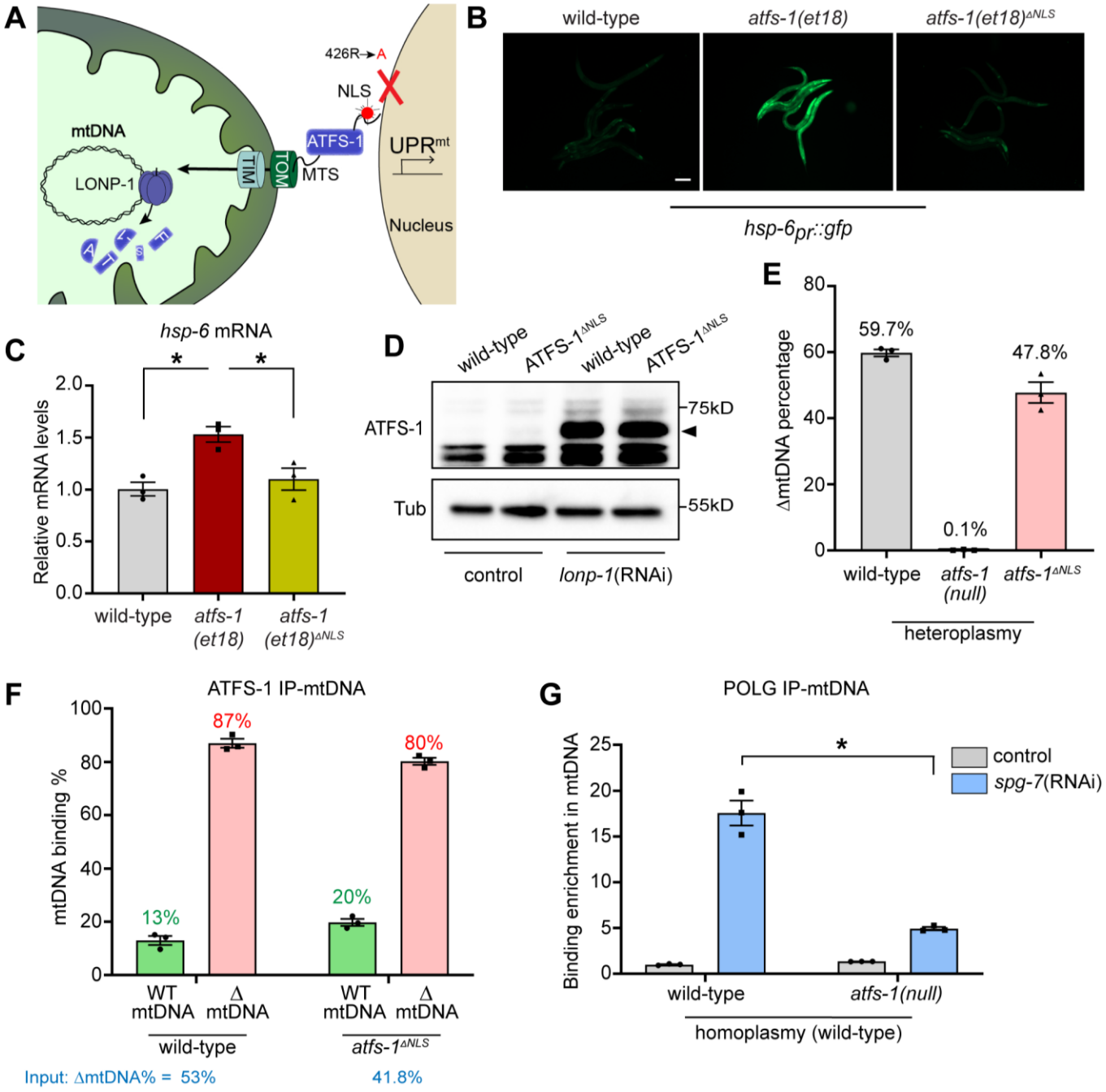
A
426R→A
NLS
mtDNA
ATFS-1
UPRmt
LONP-1
TIM
TOM
MTS
Nucleus
B
wild-type
atfs-1(et18)
atfs-1(et18)ΔNLS
hsp-6pr::gfp
C
hsp-6 mRNA
Relative mRNA levels
wild-type
atfs-1 (et18)
atfs-1 (et18)ΔNLS
D
wild-type
ATFS-1ΔNLS
wild-type
ATFS-1ΔNLS
ATFS-1
Tub
75kD
55kD
control
lonp-1(RNAi)
E
ΔmtDNA percentage
59.7%
0.1%
47.8%
wild-type
atfs-1 (null)
atfs-1ΔNLS
heteroplasmy
F
ATFS-1 IP-mtDNA
mtDNA binding %
13%
87%
20%
80%
WT mtDNA
Δ mtDNA
wild-type
atfs-1ΔNLS
Input: ΔmtDNA% = 53%
41.8%
G
POLG IP-mtDNA
Binding enrichment in mtDNA
control
spg-7(RNAi)
wild-type
atfs-1(null)
homoplasmy (wild-type)

Fig. 2. Mitochondrial-localized ATFS-1 is sufficient to maintain ΔmtDNAs. (**A**) ATFS-1$^{\Delta NLS}$/UPR^{mt} signaling schematic. (**B**) Photomicrographs of wild-type, *atfs-1(et18)* and *atfs-1(et18)$^{\Delta NLS}$;hsp-6$_{pr}$::gfp* worms. (Scale bar 0.1 mm). (**C**) Expression level of *hsp-6* mRNA in wild-type, *atfs-1(et18)* or *atfs-1(et18)$^{\Delta NLS}$* worms examined by qRT-PCR. **(D**) Immunoblots of lysates from wild-type and ATFS-1$^{\Delta NLS}$ worms raised on control(RNAi) or *lonp-1*(RNAi). ATFS-1 or ATFS-1$^{\Delta NLS}$ are indicated with an arrowhead. (**E**) ΔmtDNA quantification as determined by qPCR in heteroplasmic wild-type, *atfs-1$^{\Delta NLS}$* and *atfs-1(null)* worms. (**F**) Quantification of wild-type mtDNA and ΔmtDNA following ATFS-1 IP-mtDNA in heteroplasmic wild-type or *atfs-1$^{\Delta NLS}$* worms. Post lysis/Input ΔmtDNA ratio in wild-type worms was 53% in wild-type and 41.8% in *atfs-1$^{\Delta NLS}$* worms. (**G**) Quantification of mtDNA following POLG IP-mtDNA in homoplasmic wild-type worms and homoplasmic *atfs-1(null)* worms raised on control(RNAi) or *spg-7*(RNAi). n = 3; error bars mean ± S.E.M.; *p<0.05 (Student's t-test).

Fig. 3.

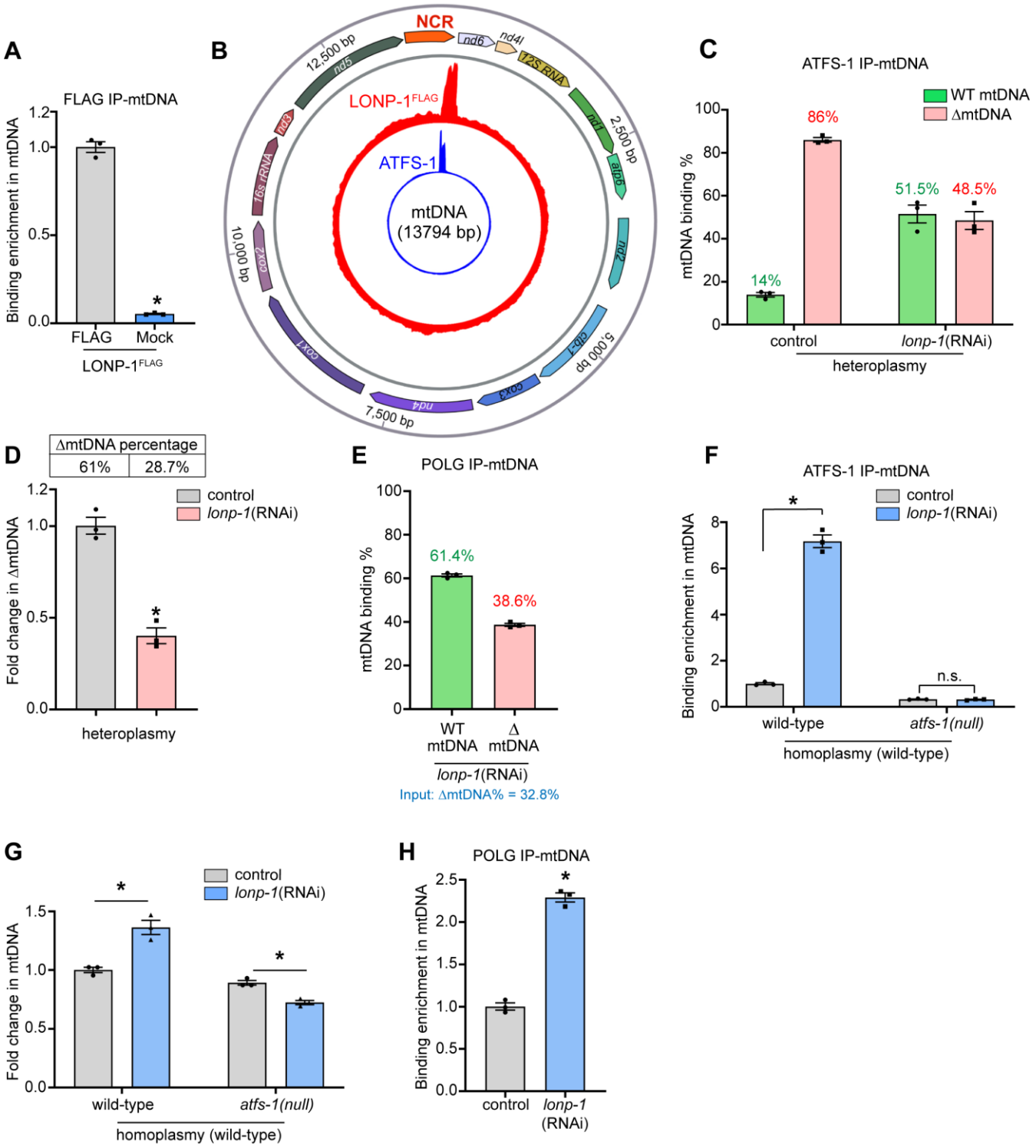
A
FLAG IP-mtDNA
Binding enrichment in mtDNA
FLAG
Mock
LONP-1FLAG
B
NCR
LONP-1FLAG
ATFS-1
mtDNA
(13794 bp)
12,500 bp
2,500 bp
5,000 bp
7,500 bp
10,000 bp
C
ATFS-1 IP-mtDNA
WT mtDNA
ΔmtDNA
mtDNA binding %
86%
14%
51.5%
48.5%
control
lonp-1(RNAi)
heteroplasmy
D
ΔmtDNA percentage
61%
28.7%
control
lonp-1(RNAi)
Fold change in ΔmtDNA
heteroplasmy
E
POLG IP-mtDNA
mtDNA binding %
61.4%
38.6%
WT mtDNA
Δ mtDNA
lonp-1(RNAi)
Input: ΔmtDNA% = 32.8%
F
ATFS-1 IP-mtDNA
control
lonp-1(RNAi)
Binding enrichment in mtDNA
n.s.
wild-type
atfs-1(null)
homoplasmy (wild-type)
G
control
lonp-1(RNAi)
Fold change in mtDNA
wild-type
atfs-1(null)
homoplasmy (wild-type)
H
POLG IP-mtDNA
Binding enrichment in mtDNA
control
lonp-1
(RNAi)

Fig. 3. Mitochondrial-localized ATFS-1-dependent mtDNA replication is negatively regulated by LONP-1. (**A**) Quantification of mtDNA in wild-type worms following IP-mtDNA using FLAG or control (Mock) antibody in LONP-1^{FLAG} worms. (**B**) ChIP-seq profile of mtDNA from homoplasmic LONP-1^{FLAG} worms raised on control(RNAi) using FLAG antibody (red). ATFS-1 ChIP-seq profile from homoplasmic worms raised on *spg-7*(RNAi) (blue) (as in Fig. 1B). (**C**) ∆mtDNA and wild-type mtDNA quantification following ATFS-1 IP-mtDNA in heteroplasmic worms raised on control(RNAi) or *lonp-1*(RNAi). (**D**) ∆mtDNA quantification in heteroplasmic worms raised on control(RNAi) or *lonp-1*(RNAi). (**E**) ∆mtDNA and wild-type mtDNA quantification following POLG IP-mtDNA in heteroplasmic worms raised on *lonp-1*(RNAi). Post-lysis/Input ∆mtDNA ratio was 32.8%. (**F**) Quantification of total mtDNA following ATFS-1 IP-mtDNA in wild-type or *atfs-1(null)* worms raised on control(RNAi) or *lonp-1*(RNAi). (**G**) Quantification of mtDNA in homoplasmic wild-type and *atfs-1(null)* worms raised on control(RNAi) or *lonp-1*(RNAi). (**H**) Quantification of total mtDNA following POLG IP-mtDNA in homoplasmic wild-type worms raised on control(RNAi) or *lonp-1*(RNAi). n = 3; error bars mean ± S.E.M.; *p<0.05 (Student's t-test).

Fig. 4.

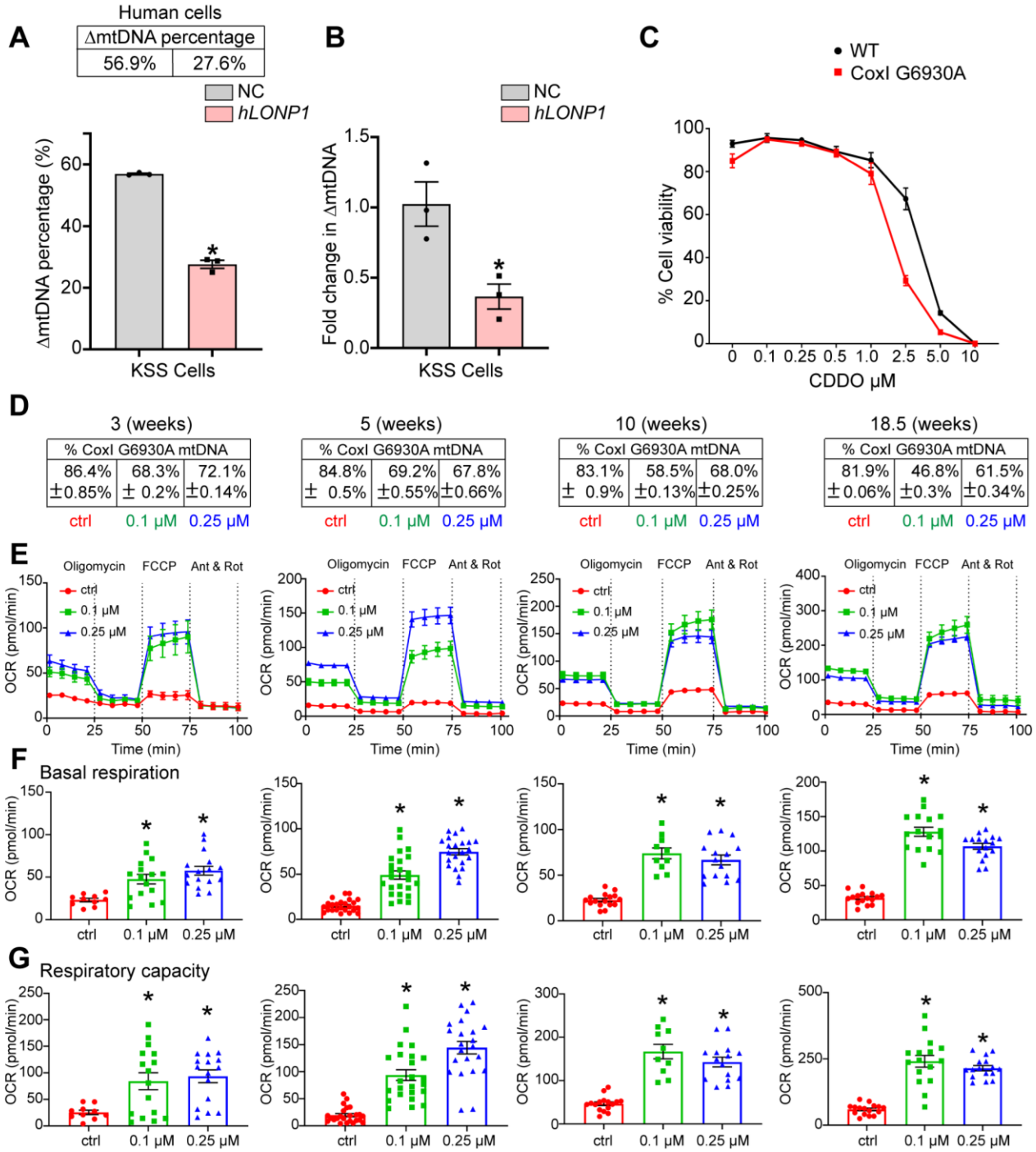
Human cells
A
ΔmtDNA percentage
56.9%
27.6%
NC
hLONP1
ΔmtDNA percentage (%)
KSS Cells
B
NC
hLONP1
Fold change in ΔmtDNA
KSS Cells
C
WT
CoxI G6930A
% Cell viability
CDDO μM
D
3 (weeks)
% CoxI G6930A mtDNA
86.4% ±0.85%
68.3% ± 0.2%
72.1% ±0.14%
5 (weeks)
% CoxI G6930A mtDNA
84.8% ± 0.5%
69.2% ±0.55%
67.8% ±0.66%
10 (weeks)
% CoxI G6930A mtDNA
83.1% ± 0.9%
58.5% ±0.13%
68.0% ±0.25%
18.5 (weeks)
% CoxI G6930A mtDNA
81.9% ±0.06%
46.8% ±0.3%
61.5% ±0.34%
ctrl
0.1 μM
0.25 μM
E
Oligomycin
FCCP
Ant & Rot
OCR (pmol/min)
Time (min)
F
Basal respiration
G
Respiratory capacity

Fig. 4. LONP1 inhibition reduces ∆mtDNAs and improves OXPHOS function in heteroplasmic human cells. (**A** and **B**) Quantification of KSS ∆mtDNA. KSS cells treated with control siRNA or *hLONP1* siRNA. (**C**) Cell viability of WT (143b) and CoxI G6930A cells exposed to various concentrations of CDDO for 72 hours. (**D**) Percentage of CoxI G6930A mtDNA in cells treated with DMSO, 0.1 μM or 0.25 μM CDDO for 3, 5, 10 or 18.5 weeks, n = 3; error bars mean ± S.E.M.; *p<0.05 (Student's t-test). (**E-G**) Oxygen consumption rates (OCR) of CoxI G6930A cells treated with DMSO, 0.1μM or 0.25μM CDDO for 3, 5, 10 or 18.5 weeks (E). (F) Quantification of basal respiration. (G) Quantification of respiratory capacity. (n >= 10, mean ± S.E.M,*p < 0.05).